Proceedings of the 1998 U.S. DOE Hydrogen Program Review

NREL/CP-570-25315

PHOTOELECTROCHEMICAL HYDROGEN PRODUCTION

Richard Rocheleau, Anupam Misra, Eric Miller
Hawaii Natural Energy Institute
School of Ocean and Earth Science and Technology
University of Hawaii at Manoa
Honolulu, HI 96822, USA

Abstract

A significant component of the U.S. DOE Hydrogen Program is the development of a practical technology for the direct production of hydrogen using a renewable source of energy. High efficiency photoelectrochemical systems to produce hydrogen directly from water using sunlight as the energy source represent one of the technologies identified by DOE to meet this mission. Reactor modeling and experiments conducted at UH provide strong evidence that direct solar-to-hydrogen conversion efficiency greater than 10% can be expected using photoelectrodes fabricated from low-cost, multijunction (MJ) amorphous silicon solar cells. Solar-to-hydrogen conversion efficiencies as high as 7.8% have been achieved using a 10.3% efficient MJ amorphous silicon solar cell. Higher efficiency can be expected with the use of higher efficiency solar cells, further improvement of the thin film oxidation and reduction catalysts, and optimization of the solar cell for hydrogen production rather than electricity production. Hydrogen and oxygen catalysts developed under this project are very stable, exhibiting no measurable degradation in 1N KOH after over 13,000 hours of operation. Additional research is needed to fully optimize the transparent, conducting coatings which will be needed for large area integrated arrays. To date, the best protection has been afforded by wide bandgap amorphous silicon carbide films.

Introduction

One of most ambitious goals of the US Department of Energy's Hydrogen Program is the large-scale production of hydrogen utilizing a renewable energy source to split water. High efficiency photoelectrochemical systems to produce hydrogen directly from water using sunlight as the energy source is one of the technologies identified by DOE to meet this mission. In order to meet DOE goals, such a system must be low cost, must operate at solar-to-chemical conversion efficiencies greater than 10% and must have long operating lifetimes. Although numerous approaches involving a variety of semiconductors have been explored since the early 1980's, progress has been slow, limited by the high voltage required to dissociate water and corrosiveness of the aqueous electrolytes. Modeling and proof-of-concept experiments conducted at UH provide strong evidence that future direct solar-to-hydrogen conversion efficiency greater than 10% can be expected with photoelectrodes fabricated from low-cost, multijunction (MJ) amorphous silicon solar cells. Based on the very thin semiconductor layers involved and on compatibility with high-throughput manufacturing processes, these systems have the potential for very low cost.

In the past, our effort was mostly focused on demonstrating the feasibility of the photoelectrochemical approach, and on improving photoelectrode efficiency by optimizing the hydrogen and oxygen catalysts. To date, solar-to-hydrogen efficiencies as high as 7.8% have been achieved using a 10.3% efficient MJ solar cell (Rocheleau et al., 1998). The relative electrochemical efficiency, the ratio of the energy content of hydrogen produced (LHV) to the maximum electrical output of the solar cells, is approximately 75% - 80% in outdoor testing for both MJ amorphous silicon on glass (from Solarex Inc.) and on stainless steel (from Energy Conversion Devices Inc.). Higher efficiency can be expected with the use of higher efficiency solar cells (13% is the current world record efficiency for stabilized amorphous silicon), further reduction in the anodic and cathodic overpotentials, and optimization of the solar cell for hydrogen production rather than electricity production. After successful demonstration of proof of concept, we are now focusing on more important issues - stability of the photoelectrode in aqueous electrolyte and development of a photoelectrode configuration amenable to scale-up.

While specialized laboratory cells using separate anodes and cathodes have been used for efficiency testing, conceptual designs of PEC reactors indicate that these configurations will not be appropriate for large integrated systems. The current research is focused on the development of transparent, conductive coatings which effectively protect the underlying semiconductor structures without causing loss of light transmission or adding significant resistive losses. To date, the best results have been obtained with wide bandgap amorphous silicon carbide films. Although these films do cause a modest increase in series resistance, this material is very transparent and in tests to date, has been very stable even in strong alkaline electrolyte.

In this report we describe progress in several parallel efforts including reactor modeling and design, catalysts development, protective film development, and outdoor testing of photoelectrochemical system.

Scope/Technical Approach

Our approach, as it has been in the past, is to compare alternate materials and system configurations using reactor modeling, and to identify and address the critical materials and photoelectrode-operation issues through extensive experiments in materials synthesis and in photoelectrode fabrication and testing. We have developed quantitative models for the photoelectrochemical production of hydrogen by combining detailed models of the performance of multijunction amorphous silicon solar cells with standard kinetic expressions describing the electrochemical reactions. We've continued our development of state-of-the-art thin film catalysts and made significant advances in the development of transparent protective thin films. Preliminary conceptual reactor designs, prepared in collaboration with NREL, indicate several important advantages of using the solar cell configurations traditionally fabricated onto metal substrates. Therefore, while continuing our strategy of working closely with the solar cell manufacturers, we are shifting our focus from the glass superstrate cells produced by Solarex to the metal substrate cells produced by Energy Conversion Devices for compatibility with the proposed conceptual designs. Use of the ECD type devices in a practical system requires development of very high quality protective films, a key focus of the current work.

Results

Loss Analysis

In 1991 we conducted a systematic analysis of semiconductor materials and photoelectrode designs (Rocheleau and Miller, 1997) to compare the potential hydrogen production rates of different semiconductor materials and in various single and multijunction configurations. This study showed that series-connected multijunction (MJ) devices could be designed to operate at voltages optimized for direct water splitting while still using a large fraction of the available solar spectrum resulting in significantly higher efficiencies than conventional single junction (single photon) systems. The multijunction approach also eliminates the need for direct contact between the semiconductor and electrolyte allowing the use of protective films to prevent corrosion. Of the photovoltaic technologies which are sufficiently developed to be considered for hydrogen production (namely, Group III-V crystalline cells and amorphous silicon) the high quality III-V materials were clearly shown to have the potential for higher solar-to-hydrogen conversion efficiencies. However, their high-cost makes them impractical for commercial PEC systems.

Surprisingly, the solar-to hydrogen conversion efficiencies predicted for the much lower cost multijunction amorphous silicon ranged up to 50% of those calculated for the best Group III-V heterojunctions. Based on the scale of manufacture under development for amorphous silicon, and on the related cost reductions predicted by the PV industry for a-Si thin-film technologies, the UH program has focused on MJ amorphous silicon devices in the development of high efficiency photoelectrodes. Figure 1 illustrates the modeling of multijunction amorphous silicon photoelectrodes as a solar cell structure series-connected with an electrochemical load. This analysis includes the current-dependent overpotentials

due to charge transfer kinetics at the electrode surfaces in addition to resistances for the potential drop due to ion transport through the electrolyte. Details of the a-Si solar cell modeling as well as assumptions used in the analysis of the electrochemical kinetics have been described elsewhere (Rocheleau and Vierthaler,1994; Rocheleau,Tun and Hegedus, 1997; Miller, 1996). The predicted hydrogen-production rate based on an integration of actual data into the photoelectrode model is shown in Figure 2, where the JV curve of a triple junction Solarex solar cell (10.3% stabilized) is superimposed with a measured electrochemical operating curve. As described later, the indicated 7.8% solar-to hydrogen efficiency of this system has been verified in experimental results. Small area amorphous silicon solar cells with 13%-stabilized efficiency have been developed (Yang, et al., 1997). Although solar cells of this efficiency level have not yet been made available for testing, use of this quality device in a hydrogen production system using the thin film catalysts developed at UH would be expected to yield solar-to-hydrogen efficiencies greater than 10%.

Reactor Design

Figure 3 shows a conceptualized picture of a photoelectrochemical reactor for hydrogen production utilizing multijunction (MJ) amorphous silicon photoelectrodes. This reactor is based on designs developed in collaboration with NREL, Energetics, and Distributed Utility Associates during the fall of 1997. Figure 4, shows a conceptualized cross section of the active MJ photoelectrode element. The active cell may be configured for light through the p-layer (pinpinpin-as shown), or in the alternate configuration for light through the n-layer (nipnipnip). Photogenerated electrons drift, under the influence of the internal fields, toward the n-layer while the holes drift toward the p-layer for collection. A key difference of this photoelectrochemical configuration, compared with the solid-state solar cell configuration is absence of the lateral current collection required in solar cells. We believe that significant cost advantage of the integrated photoelectrochemical system over conventional PV-electrolysis (i.e., solid-state solar cells driving electrolyzers) can be realized since the integrated system can take advantage of the simpler processing and reduced materials constraints allowed when current is transferred directly through, rather than collected laterally in the transparent contact.

The photoelectrode structure (Figure 4) consists of a MJ amorphous silicon solar cell deposited directly onto a supporting substrate. This substrate may be conductive such as the stainless steel used in the ECD cell configuration, or it may be a nonconductive material. If the latter is used, additional processing is necessary to provide a conductive path between the backside of the cell and the back-side catalyst. In the configuration shown, the contact/membrane is assumed to be conductive, the solar cell is grown nipnipnip so that light is incident on the p-layer, the catalyst on the back side drives the hydrogen reaction (e.g. CoMo or similar material) and the front p-side includes a transparent protective coating, and a low overpotential oxygen evolution catalysts (e.g. Fe:NiOx). In this configuration, the backside hydrogen electrode is not required to be transparent and is not in direct contact with the semiconductor and thus is easily processed. In the case of ECD cells on stainless steel substrates, we have successfully demonstrated the performance of this element of the system using sputter deposited CoMo.

Since ions involved in the electrochemical reactions are not transported through the solar cell, a path for ionic continuity must be provided. Figure 4 depicts a configuration in which the substrate is physically attached to an ionic transport membrane to provide electrical continuity around the cell. However, if a suitable ionic conducting material can be developed, the back contact and solar cell could be deposited directly on the membrane, simplifying fabrication of the system. These design/synthesis issues are to be addressed next year. For the configuration shown, stability of the hydrogen electrode is determined by the hydrogen catalyst. Per the results discussed in the next section, stable, high activity thin film hydrogen catalysts have already been developed at UH. Stability at the front (p) interface is more complicated, requiring a thin layer which fully protects the underlying semiconductor while retaining its transparency and conductivity, and is compatible with the catalyst. While progress has been made this year, we feel this is the critical problem to be solved if a practical low-cost PEC system is to be developed. Progress to date is described later in this report.

Elements of the reactor system include arrays of photoelectrode modules, separation systems to remove hydrogen and oxygen from the electrolyte, storage tanks and fluid pumps etc. It is envisioned that the PEC reactor will operate at modest solar concentration, 5 to 10 suns, taking advantage of the fact that carrier transport directly through the transparent window (vs. the lateral current collection) reduces series resistance. Properly designed, the cylindrical reactor body itself could provide some or all of the concentration. The reactor is easily expandable by adding additional arrays of photoelectrodes. It is desirable to allow the photoelectrode to be changed out to accommodate replacements should failure occur or new photoelectrodes with better performance be discovered. Since only water is consumed in the reaction, makeup is simple and could be accomplished using simple gravity feed.

Catalyst Development

The University of Hawaii has made considerable progress in the development of stable high performance catalysts for hydrogen-producing planar photoelectrodes. Reactively-sputtered layers of Fe:NiOx with high activity for oxygen evolution have been demonstrated and reported in detail elsewhere (Miller and Rocheleau, 1997; Miller and Rocheleau, 1997). Although under certain processing conditions good transparency is maintained in these oxide films, this has come at the expense of reduced activity. Additional improvements to optimize both transparency and OER activity are desired. UH has also demonstrated reactively-sputtered films of cobalt/molybdenum with excellent stability and high hydrogen evolution activity. Since these thin film catalysts are in direct contact with the electrolyte, stability under normal operating conditions is essential.

Long term stability testing of both oxygen and hydrogen catalysts was conducted by mounting samples of Fe:NiOx (oxygen catalyst) and CoMo (hydrogen catalyst) on a specially designed Plexiglas PEC cell using Teflon gaskets. The stability test consists of monitoring electrode potentials at constant current density of 20 mA/cm^2 in 1 N KOH made from ACS grade KOH and commercially available drinking water. Use of low grade chemical and water was required

to keep the cost of electrolyte low, however use of dirty electrolyte requires very stable oxygen and hydrogen catalysts to be developed and utilized. Figure 5(a) shows the total cell potential (V_{cell}) and the anodic (Fe:NiO_X) half cell potential for the 13,600 hour test at a continuous current of 20 mA/cm^2. Although there is some variation in both the total and half cell potentials during the testing, there is no consistent trend toward higher potential, i.e. degraded electrodes for either. The constant anodic half cell potential is indicative of a stable Fe:NiOx OER catalyst. The constant difference between the total cell and half cell potentials is indicative of stable CoMo HER catalyst. The high total cell potential includes a significant IR drop through the electrolyte due to the large anode/cathode separation in this particular test cell, however, the catalytic activity of the OER and HER are similar to our best materials previously reported.

Figure 5(b) shows the anodic half cell (vs SCE) and total cell current-potential (JV) sweeps at the start of and following 13600 hrs at a constant current density of 20 mA/cm^2. Consistent with the results in Figure 5(a) the oxygen catalyst (nickel iron oxide) shows very stable performance. The total cell potential actually shows some improvement indicating improvement in the CoMo. The additional experiments evaluating properties of electrolyte at various times during test indicate that the improvement of CoMo is due to the hydrogen reduction and is not related to the change in electrolyte properties. Molybdenum is known to oxidize readily during deposition and during stand alone periods. A constant hydrogen evolution on CoMo catalyst seems to remove oxygen and improve the catalytic action. The hydrogen catalyst was found to recover from damage from the oxidation during a 5 day stand alone non-operational period. Data indicate that for commercial system, one would either need cathodic protection or artificial light during night hours. The long term testing of these two electrodes is continuing.

Previously, we have improved the performance of the oxygen catalysts by introducing transition metals into the sputtered NiOx films. Similar experiments were conducted during this phase of the project in an effort to further reduce the overpotentials associated with the hydrogen evolution reaction. The replacement of Co by Ni was found to reduce the overpotential in 1N KOH by approximately 50 mV as shown in Figure 6. The improvement in the NiMo during the first 1500 seconds of operation is believed to be due to removal of surface oxide under the reducing conditions found at the anode. Experiments are underway to further optimize the hydrogen catalyst and to characterize the surface reaction.

Protective Coatings

Protective coatings for the surface of the photoelectrode exposed to electrolyte and through which the light passes (top p-layer in the configuration shown in Figure 4) must be transparent, corrosion resistant and pinhole free, and electrically conducting. A literature search of potential materials meeting these requirements included zinc oxide (ZnOx), indium tin oxide (ITO), tin oxide (SnOx), doped and undoped amorphous silicon carbide (a-SiC:H), and diamond and diamond-like carbon (DLC) films. All of these films are transparent and can be doped to become conducting. The choice of suitable protective film is then mainly

dependent on its chemical inertness, ease of processing and physical protection for the underlying semiconductor layers (e.g. ability to deposit pinhole free). ZnOx films are reported to be unstable in 1 N KOH and so were not included in the corrosion testing. The literature indicates that SnOx films are more stable than either the ITO or ZnOx films. Commercial samples of SnOx were obtained and tested in our electrochemical cells. These films dissolved in 1 N KOH within a day. Since alloying or the addition of dopants can play an important role in determining the electrochemical behaviors of a protective film, it still may be possible to develop a stable SnOx film in the future by adjusting the film composition. ITO films of variable resistivities are currently being deposited using the same sputtering system used for catalyst deposition. Testing of the electrochemical/corrosion characteristics is planned but has not yet started.

The best results to date have been obtained using amorphous silicon carbide films deposited using plasma enhanced chemical vapor deposition, a process which has been described in some detail in previous reports (Rocheleau, Miller and Misra, 1997). It was previously reported that a-SiC:H films deposited under conditions of high hydrogen dilution were physically harder and were more resistive to corrosion than films deposited from undiluted mixtures of silane and methane.

Figure 7 shows the anodic polarization curve for a bare nickel substrate and for four Ni substrates coated with a-SiC:H. The polarization curves were obtained by sweeping from the corrosion potential into the anodic region in 1N KOH. Data were taken at an interval of 0.01 V although, for clarity, data are shown only every 0.20 volts. The a-SiC:H was deposited at silane to methane ratios ranging from(4:6 to 1:9). At a deposition pressure of 0.5 torr, the bandgap of the a-SiC:H films increased from 2.0 to 2.25 eV as the methane fraction in the feedgas increased from 60% to 90%. The bandgap was further increased, to 2.72 eV, when the film was grown from the gas with the 1:9 silane to methane ratio at a reduced pressure of 0.133 torr. We speculate that the increase in bandgap is the direct result of greater C incorporation into the films. Confirming measurements will be conducted. As the bandgap increased, the films became significantly more transparent in the visible spectrum. Figure 7 shows that as the bandgap is increased, the silicon carbide films also become more corrosion resistant. Since the underlying nickel substrate is more noble than a-SiC:H in KOH solution, the anodic polarization below 0.1 Vsce represents the characteristic behavior of the a-SiC:H films in KOH electrolyte. With the increase in the methane concentration and bandgap, the samples show systematic decrease in the corrosion current density and become more noble. The increase in the current density at about 0.5 Vsce is due to oxygen evolution from the samples.

Figure 8 shows the electrochemical behavior of a Ni substrate coated with the intrinsic 2.25eV a-SiC:H film held at constant current density of 20mA/cm^2 in 1 N KOH. Any dissolution of the films resulting in exposure of the underlying Ni should be accompanied by a decrease in the potential (Vsce approaching substrate potential). None was observed. Visual inspection of the film after 120 hours of corrosion testing (Figure 9a) showed no evidence of dissolution or thinning of the film. The intrinsic a-SiC:H is extremely stable in the 1N KOH.

While the transparency and corrosion resistance of the a-SiC:H films increases as the bandgap increases (e.g. with greater carbon incorporation) the resistivity of the film, hence the series resistance loss in photoelectrodes using these protective films increases. A select number of films were produced with boron doping to see if resistance could be reduced while maintaining transparency and chemical stability. Figure 10 shows the anodic polarization curve of a boron doped film with an optical bandgap of 2.0 eV. Although showing a higher corrosion current and being less noble than the very high bandgap intrinsic film shown for comparison in Figure 10, comparison to Figure 7 shows the boron doped films to be as or slightly more corrosion resistant than intrinsic films of comparable bandgap. The long term stability of the p type a-SiC:H:B films under anodic bias in 1 N KOH is shown in Figure 11. After 20 hours the half cell potential approached the substrate potential indicating dissolution of the film. This was confirmed by visual inspection (Figure 9b). Additional experiments will be conducted to simultaneously optimize the chemical resistance and electrical properties of the film.

To date, all electrochemical testing has been conducted in 1N KOH which was selected due to the low overpotential and good stability of the catalysts in KOH. Since the reactivity of the protective film will change with electrolyte, additional improvements in the performance of the films may result by changing the composition of the electrolyte. Development of a more neutral, less corrosive electrolyte which maintains the low overpotential of the sputter deposited catalysts is a suggested area of research for next year.

Our research plan calls for the installation of an ASTEX reactor to allow the evaluation of diamond-like carbon films. Funds from other sources have been obtained to assist in the installation of this equipment and laboratory space has been acquired. Progress in this area will be reported later.

Bilayer structures including protective a-SiC:H and Fe:NiOx catalyst films were also fabricated and characterized. Corrosion testing of these bilayers was again conducted at constant current of 20 mA/cm^2 in 1 N KOH. Figure 12 shows the bias required to maintain constant current on a Ni/i-SiC:H/Fe:NiOx multilayered sample over the 140 hour test. The initial potential is slightly higher than that of Fe:NiOx on Ni due the to series resistance introduced by the intrinsic a-SiC:H. Although both films used in this structure are stable by themselves (e.g. on Ni) the half cell potential of the bilayer gradually increases during the 140 hour test. Examination of the electrolyte and films showed that this rise was caused by poor adhesion of the oxygen catalyst (Fe:NiOx) to the amorphous silicon film, causing a decrease in the area of the catalytic film. Additional experiments are planned to improve bonding between these materials.

Similar testing was conducted using boron doped films, i.e. Ni/p-SiC:H:B/Fe:NiOx. In contrast to the bilayer with the intrinsic film, the boron doped p-type SiC film is not stable in KOH. Stability of this structure thus depends on the ability of the Fe:NiOx to protect the underlying films. The initial potential is very close to that of Fe:NiOx alone, as expected for the more conductive boron doped silicon film. However, as shown in Figure 13, there again is a gradual increase in the potential, this time, toward the potential of the Ni substrate indicating corrosion of the a-SiC:H:B film. The corrosion of this film is

presumably caused by pinholes in Fe:NiOx film and/or poor adhesion of Fe:NiOx to the a-SiC. Figure 14 shows the photograph of the two bilayers after corrosion testing. Adhesion of the FeNiOx was a problem in both cases. We plan on exploring remedies to this problem in the future with systematic test runs and optimization of the deposition process.

Outdoor Testing

Previously we have reported an outdoor solar-to-hydrogen conversion efficiency of 7.8% using photoelectrodes fabricated from glass/CTO/pin-pin-pin triple junction a-Si solar cell provided by Solarex Inc. The experimental efficiency was consistent with those predictions from the load line analysis. The hydrogen production efficiency of photoelectrodes was 7.8%, which was about 77% of the efficiency of the triple junction cell (Rocheleau et al., 1998).

Triple junction a-Si solar cells on stainless steel substrates are available from ECD Inc. in the configuration ss/nip-nip-nip/CTO. As already discussed, this configuration offers potential design advantages and is expected to be more applicable for commercial reactors. Outdoor testing of photoelectrochemical cells constructed from these solar cells was conducted using same setup as described in previous reports (Rocheleau, Miller and Misra, 1997). Figure 15 shows the JV behavior of the triple junction solar cell available to us at the time of this test. Insolation was monitored using a standard crystalline silicon cell (pn junction) mounted onto the reactor in the same plane as the photoelectrode. A maximum solar cell efficiency of 8.7% was measured for the batch of cells cut from a sheet from their pilot scale reactor.

Figure 16 shows the result of a one hour outdoor test performed between 1:00 PM and 2:00 PM on a clear day. The photoelectrode configuration was CoMo catalyst deposited directly on the stainless steel substrate with an nip-nip-nip solar cell coated with ITO. Electrical leads were attached to the ITO and to a separate Fe:NiOx/Ni anode. The line shows the insolation on the cell measured with our secondary standard, the crystalline cell. The symbols (cross: left ordinate) show the current passing between the anodic and cathodic surfaces of the photoelectrode. The middle inset of figure 15 shows the net solar-to-hydrogen conversion efficiency of the photoelectrode as a function of time, approximately 6.6%. The ratio of the hydrogen conversion efficiency to solar cell efficiency is approximately 78% as shown in the inset at top of Figure 16. This is consistent with the electrochemical efficiency obtained with the Solarex cell in the earlier testing.

Summary and Plans

Direct solar-to-hydrogen conversion efficiency of photoelectrodes fabricated from low cost triple junction amorphous silicon solar cells has been shown to be about 78% that of solar cell efficiency. Results from outdoor tests on commercially available multijuction cells in two different configurations are consistent with each other and also with the loss analysis

model capable of predicting PEC efficiency. Thin film oxygen and hydrogen catalyst films have been shown to be very stable over 13,000 hours in strong alkaline electrolyte. Further improvement in the solar-to-hydrogen efficiency are expected with higher efficiency solar cells, better catalysts, and use of MJ cells optimized for hydrogen production. With proof of concept efficiency experiments completed, we are now focusing on long term stability issue of the system which, we believe, is the most critical materials issue remaining to be solved. Substantial progress has been made in the development of stable, protective a-SiC:H films. Intrinsic films show no degradation in 1N KOH. However, further optimization of transparency and electrical properties are needed. In order to fabricate a highly stable photoelectrode, we plan to continue our research into the development of stable conducting transparent protective films and to expand the effort to include the development of less corrosive electrolytes. We will continue to explore multilayer structures to take advantage of the best features of each material.

Increased attention to the development of conceptual and engineering designs of photoelectrochemical systems is needed to insure that the materials problems identified for research are relevant to the eventual production of commercial systems.

Acknowledgments

We wish to thank the US Department of Energy for support of this work under Grant DE-FG04-94AL85804. We also wish to Solarex Inc. and Energy Conversion Devices for amorphous silicon samples. We also wish to thank Maggie Mann of NREL and Phil DiPietro of Energetics for their useful discussions and input in the development of conceptual designs for large scale systems.

References

Miller, E. L., and R. E. Rocheleau. 1997. "Electrochemical Behavior of Reactively Sputtered Iron-doped Nickel Oxide" J. Electrochem. Soc. 144(9):3072-3077.

Miller, E. L., and R. E. Rocheleau. 1997. "Electrochemical and Electrochromic Behavior of Reactively Sputtered Nickel Oxide" J. Electrochem. Soc. 144(6):1995-2003.

Miller, E. L., 1996. "A Study of the Electrochemical Behavior and Optical Properties of Reactively-sputtered Nickel Oxide and Nickel-Iron Oxide" University of Hawaii PH.D. Dissertation.

Rocheleau, R. E., and Miller, E. L. 1997. "Photoelectrochemical Production of Hydrogen: Engineering Loss Analysis" Int. J. Hydrogen Energy. 22(8):771-782.

Rocheleau, R. E., Miller, E. L., and A. Misra. 1997. " Photoelectrochemical Hydrogen Production" *Proceedings of the 1996 U.S. DOE Hydrogen Program Review,* 345-358. Miami FL. U.S. Department of Energy.

Rocheleau, R. E., Miller, E. L., and A. Misra. 1998. "High-Efficiency Photoelectrochemical Hydrogen Production using Multijunction Amorphous Silicon Photoelectrodes" Energy and Fuels. 12: 3-10.

Rocheleau, R. E., Tun, M., and S. S. Hegedus. 1997. "Analysis and Optimization of High Efficiency Multijunction a-Si:H Solar Cells" *Proceedings of the 26th IEEE Photovoltaic Specialists Conference*, 703-706. Anaheim CA: IEEE.

Rocheleau, R.E., and Vierthaler, M. 1994. "Optimization of Multijunction a-Si:H Solar Cells Using an Integrated Optical/Electrical Model." *Proceedings of the 21st World Conference on Photovoltaic Energy Conversion* , 567-570. Honolulu HI: IEEE.

Yang, J., Banerjee, A., Glatfelter, T., Sugiyama, S., and S. Guha. 1997. "Recent Progress in Amorphous silicon Alloy Leading to 13% Stable Cell Efficiency" *Proceedings of the 26th IEEE Photovoltaic Specialists Conference*, 703-706. Anaheim CA: IEEE.

FIGURE CAPTIONS

Figure 1: Analytical model for photo-electrolysis based on a solid-state photogenerator (shown for a triple-junction device) driving an electrochemical load.

Figure 2: Load line analysis showing the operating point of a photoelectrochemical cell as the intersection of the JV curve of the photocell and the load curve of the electrochemical components.

Figure 3: Conceptual design of photoelectrochemical reactor for hydrogen production.

Figure 4: Cross section of multijunction photoelectrode for direct water splitting.

Figure 5: Long term stability test results for sputtered Fe:NiOx and CoMo catalyst films at constant current of 20 mA/cm^2 in 1N KOH.

Figure 6. Electrochemical behavior of sputter deposited CoMo and NiMo thin films at constant current of 20 mA/cm^2 in 1N KOH.

Figure 7. Anodic polarization scans of a-SiC:H films deposited on Ni substrate in 1N KOH.

Figure 8. Electrochemical behavior of a-SiC:H on Ni under anodic bias in 1N KOH.

Figure 9: Photographs of a-SiC:H, boron doped a-SiC:H and SnO think films after exposure to 1N KOH.

Figure 10. Comparison of the anodic corrosion of boron doped and intrinsic a-SiC:H films on Ni in 1N KOH.

Figure 11. Electrochemical behavior of boron doped a-SiC:H on Ni under anodic bias at constant current density in 1N KOH.

Figure 12. Electrochemical behavior of Fe:NiOx/intrinic a-SiC:H bilayers on Ni under anodic bias 1N KOH.

Figure 13. Electrochemical behavior of Fe:NiOx/boron doped a-SiC:H bilayers on Ni under anodic bias 1N KOH.

Figure 14. Photographs of bilayer films (catalyst/amorphous silicon carbide) showing poor adhesion of Fe:NiOx to amorphous silicon film.

Figure 15. JV behavior of ECD solar cell used to fabricate CoMo/ss/nip-nip-nip-Fe:NiOx photoelectrode.

Figure 16. Photoelectrode current density (x's) and solar-to-hydrogen conversion efficiency (middle inset), and electrochemical efficiency (top inset) during a one hour outdoor test on a clear afternoon (measured insolation shown by line in lower plot).

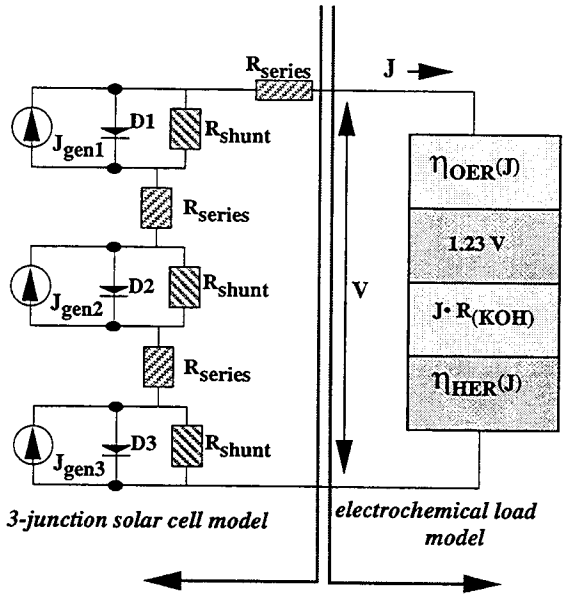
R_series
J
D1
J_gen1
R_shunt
R_series
D2
J_gen2
R_shunt
R_series
D3
J_gen3
R_shunt
V
η_OER(J)
1.23 V
J• R_(KOH)
η_HER(J)
3-junction solar cell model
electrochemical load model

Figure 1

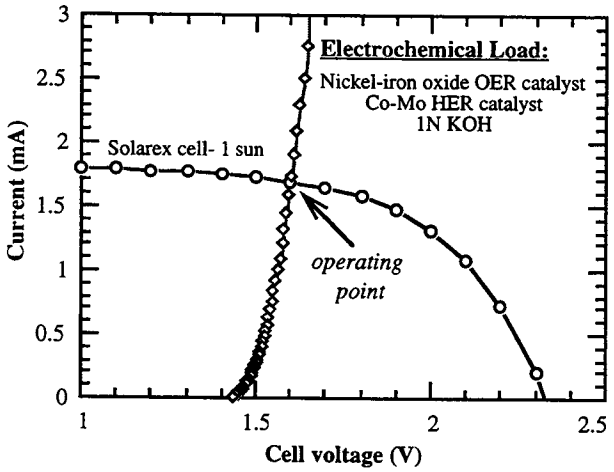
Electrochemical Load:
Nickel-iron oxide OER catalyst
Co-Mo HER catalyst
1N KOH
Solarex cell- 1 sun
operating point
Current (mA)
Cell voltage (V)
3
2.5
2
1.5
1
0.5
0
1
1.5
2
2.5

Figure 2

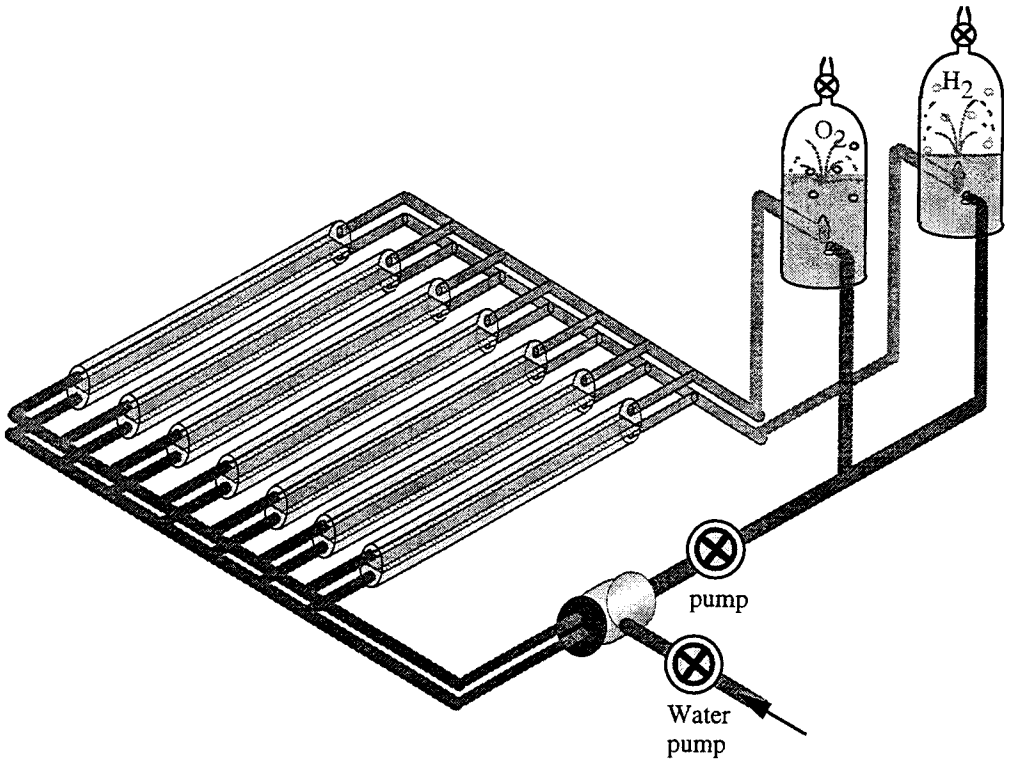

Figure 3

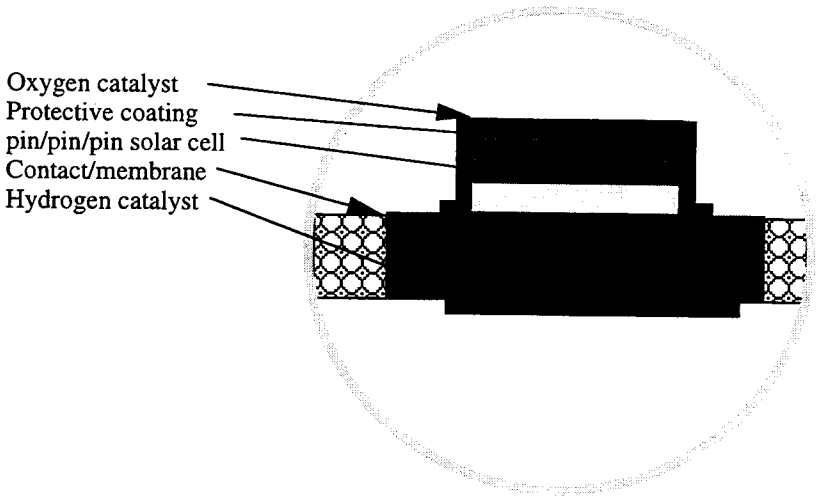
Oxygen catalyst
Protective coating
pin/pin/pin solar cell
Contact/membrane
Hydrogen catalyst

Figure 4

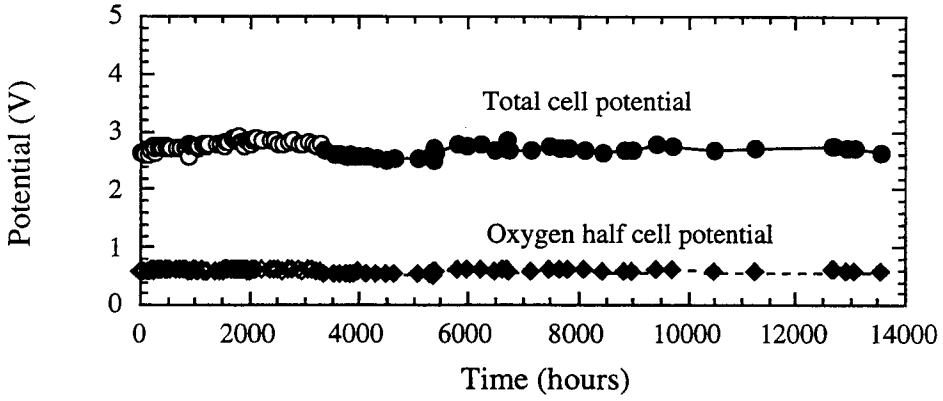
Potential (V)
Total cell potential
Oxygen half cell potential
Time (hours)

(a)

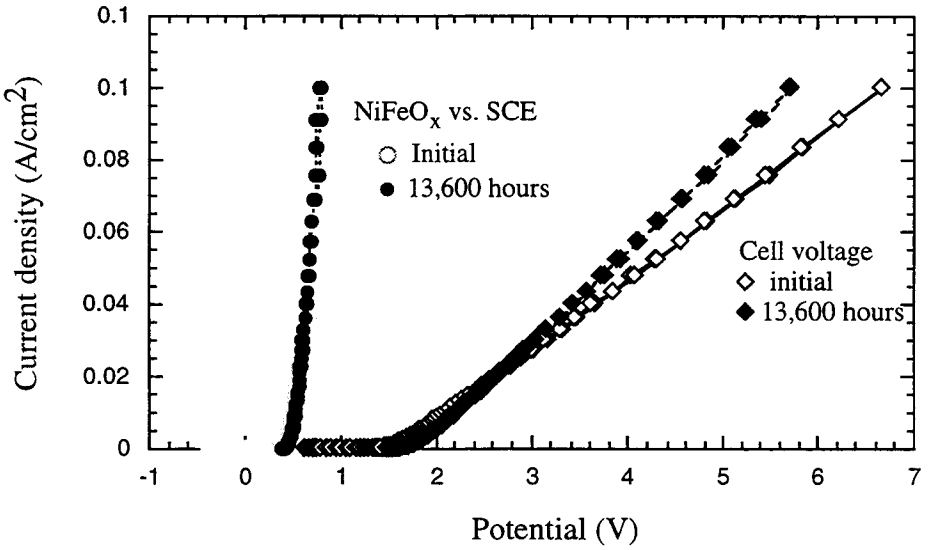
Current density (A/cm2)
NiFeOx vs. SCE
Initial
13,600 hours
Cell voltage
initial
13,600 hours
Potential (V)

(b)

Figure 5

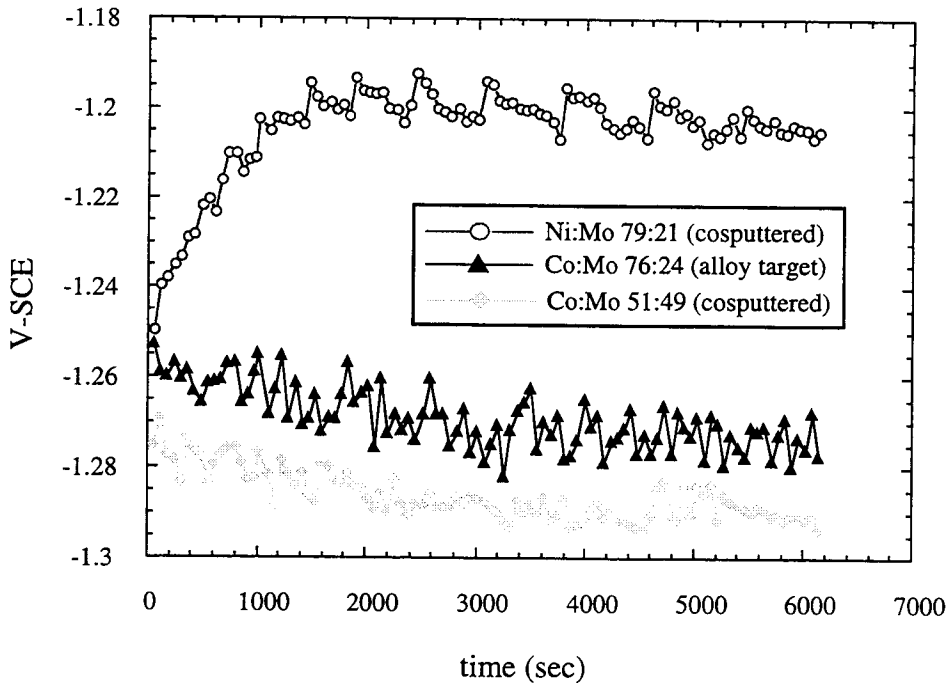
-1.18
-1.2
-1.22
-1.24
-1.26
-1.28
-1.3
V-SCE
0
1000
2000
3000
4000
5000
6000
7000
time (sec)
Ni:Mo 79:21 (cosputtered)
Co:Mo 76:24 (alloy target)
Co:Mo 51:49 (cosputtered)

Figure 6

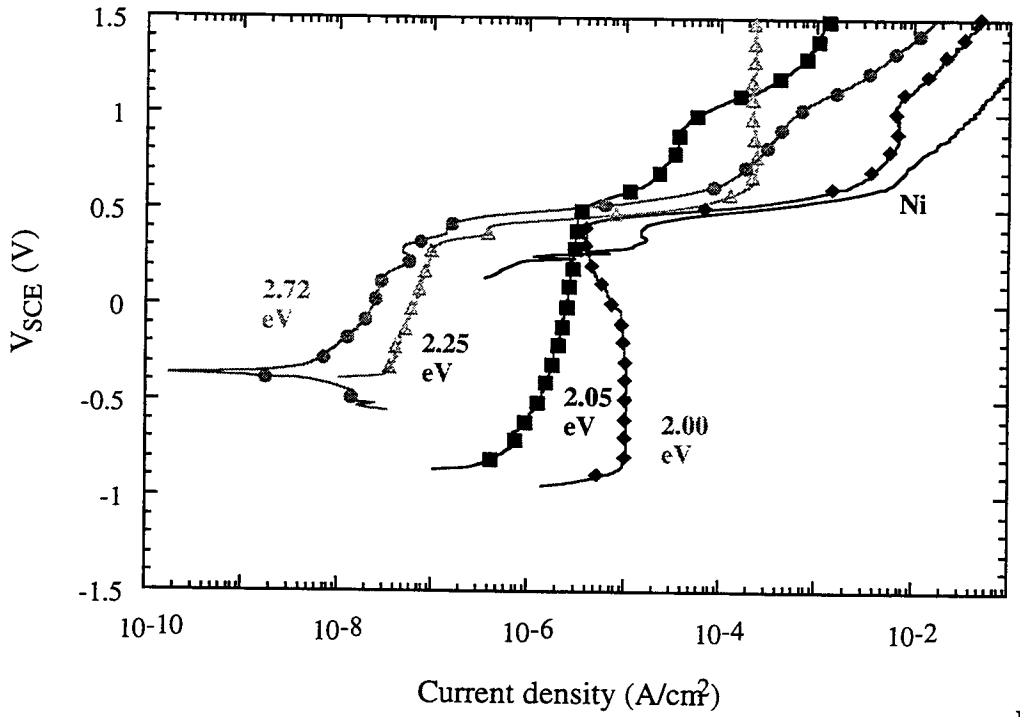
1.5
1
0.5
0
-0.5
-1
-1.5
V_{SCE} (V)
10-10
10-8
10-6
10-4
10-2
Current density (A/cm^2)
2.72 eV
2.25 eV
2.05 eV
2.00 eV
Ni

Figure 7

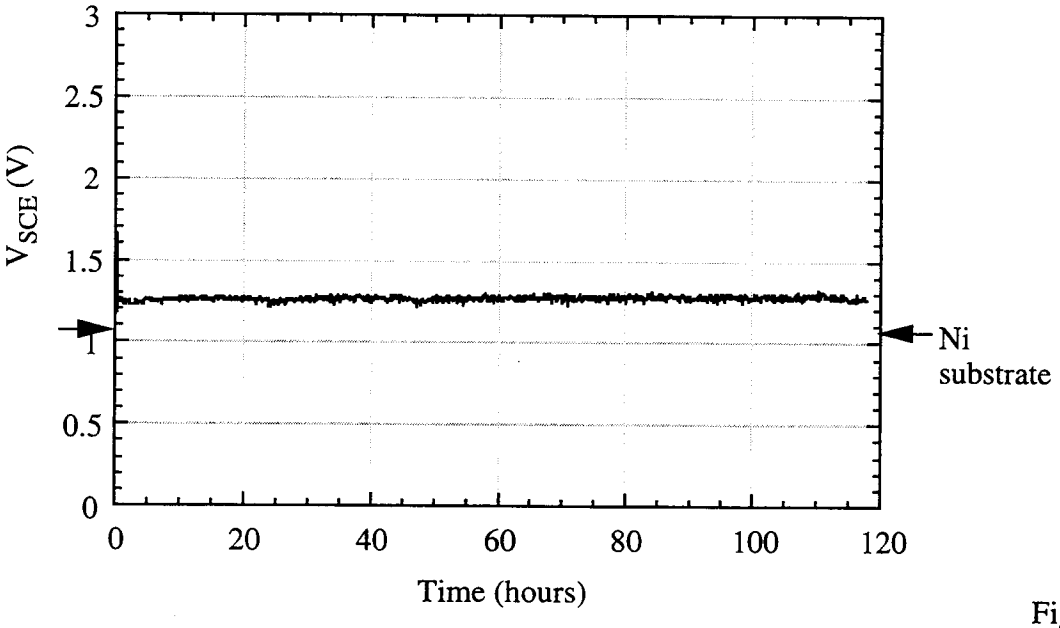
3
2.5
2
1.5
1
0.5
0
V_{SCE} (V)
0
20
40
60
80
100
120
Time (hours)
Ni
substrate

Figure 8

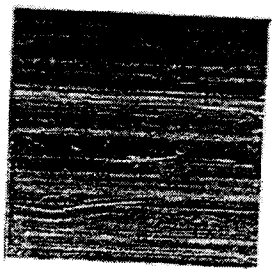

Intrinsic a-SiC:H
(5 days)

P-type a-SiC:H:B
(2 days)

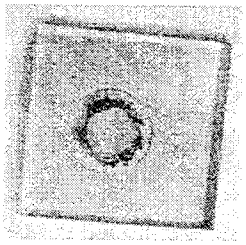

Conducting SnO
(1 day)

Figure 9

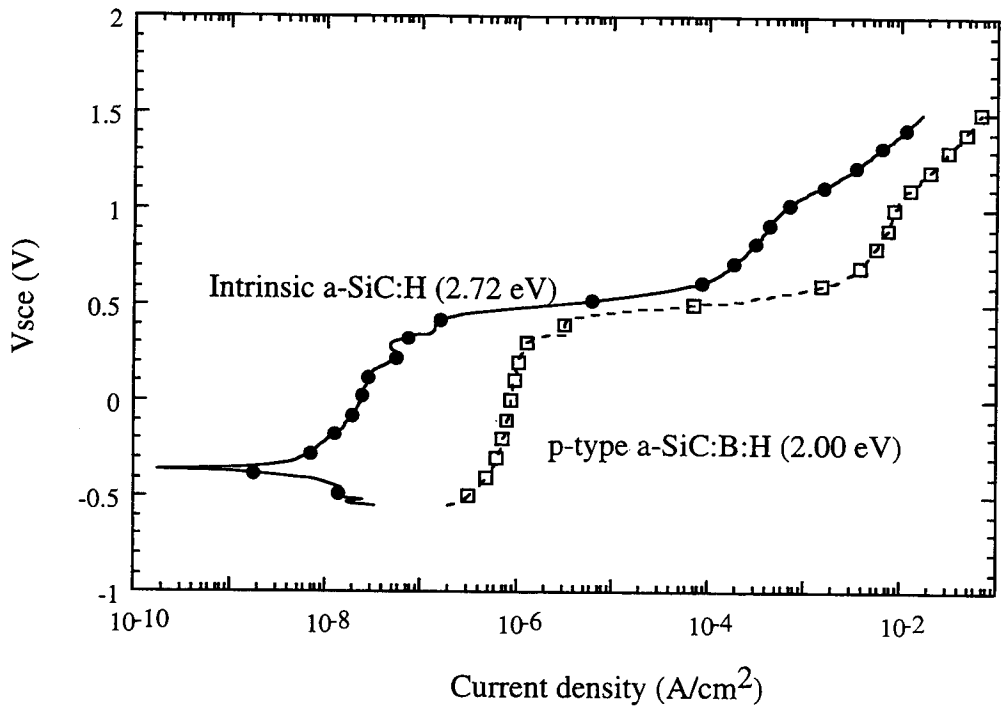
2
1.5
1
0.5
0
-0.5
-1
Vsce (V)
Intrinsic a-SiC:H (2.72 eV)
p-type a-SiC:B:H (2.00 eV)
10-10
10-8
10-6
10-4
10-2
Current density (A/cm2)

Figure 10

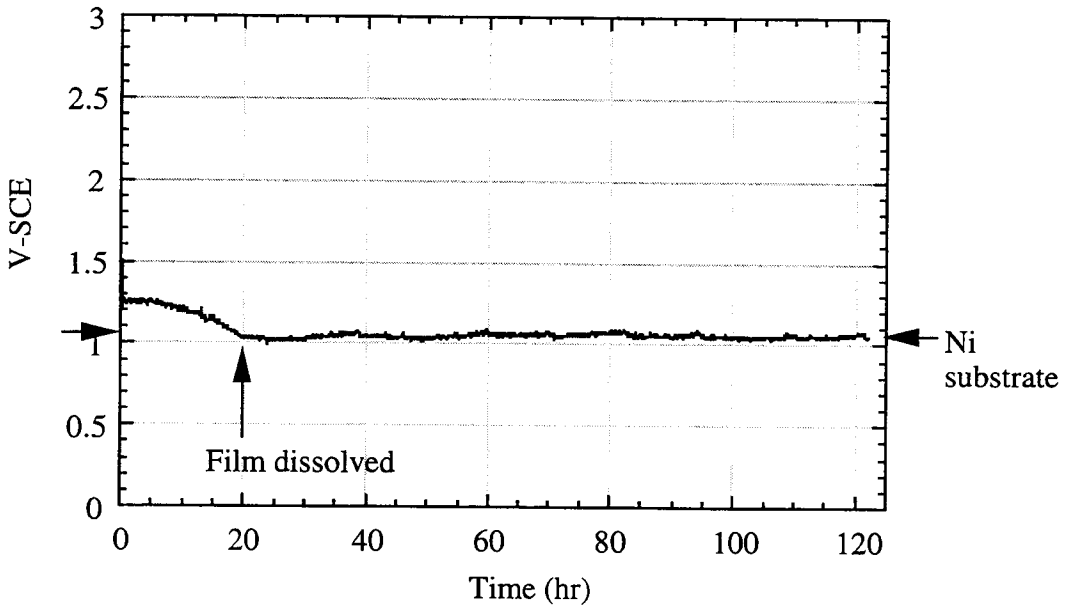
3
2.5
2
1.5
1
0.5
0
V-SCE
0
20
40
60
80
100
120
Time (hr)
Film dissolved
Ni
substrate

Figure 11

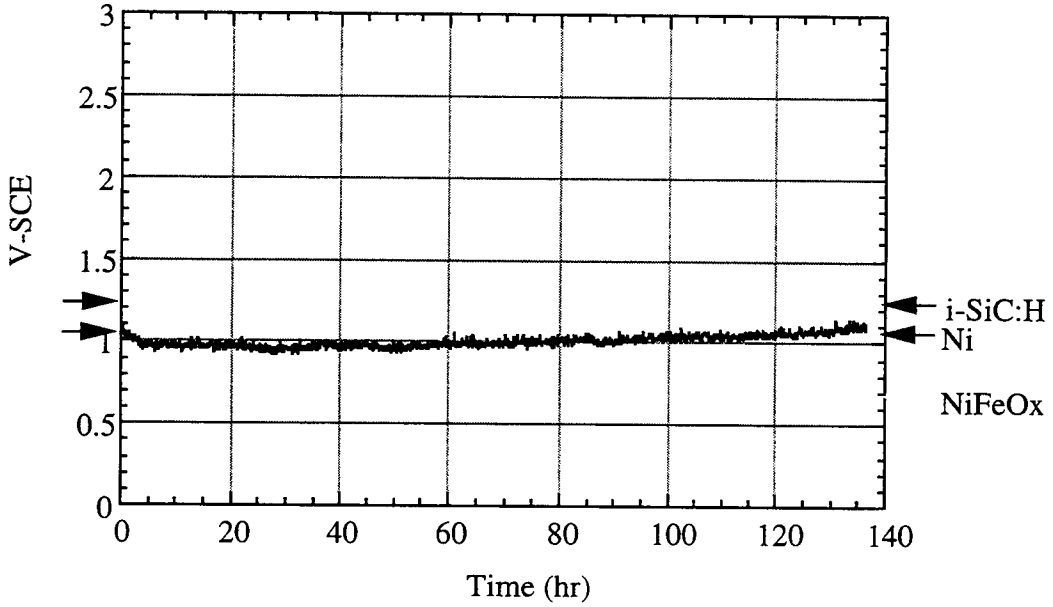
V-SCE
3
2.5
2
1.5
1
0.5
0
0
20
40
60
80
100
120
140
Time (hr)
i-SiC:H
Ni
NiFeOx

Figure 12

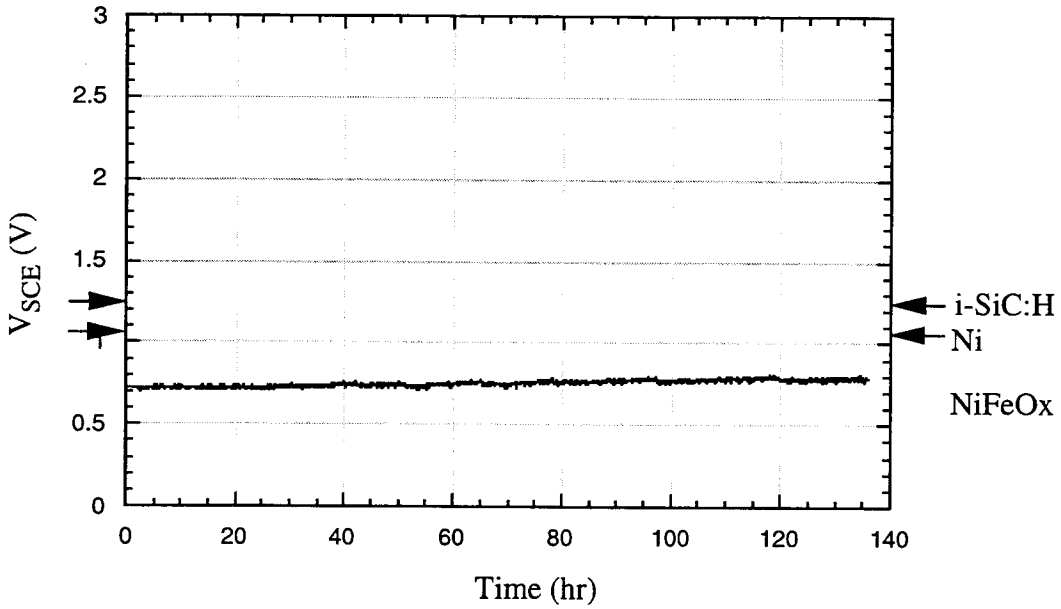
3
2.5
2
1.5
0.5
0
V_{SCE} (V)
0
20
40
60
80
100
120
140
Time (hr)
i-SiC:H
Ni
NiFeOx

Figure 13

Ni/i-SiC:H/NiFeOx

Ni/p-SiC:H:B/NiFeOx

Figure 14

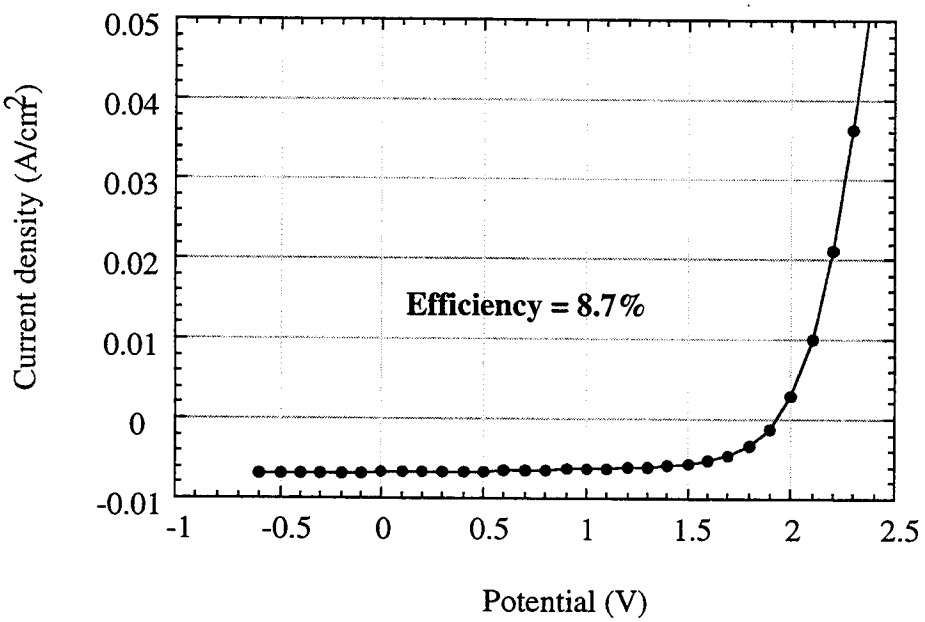
0.05
0.04
0.03
0.02
0.01
0
-0.01
Current density (A/cm2)
Efficiency = 8.7%
-1
-0.5
0
0.5
1
1.5
2
2.5
Potential (V)

Figure 15

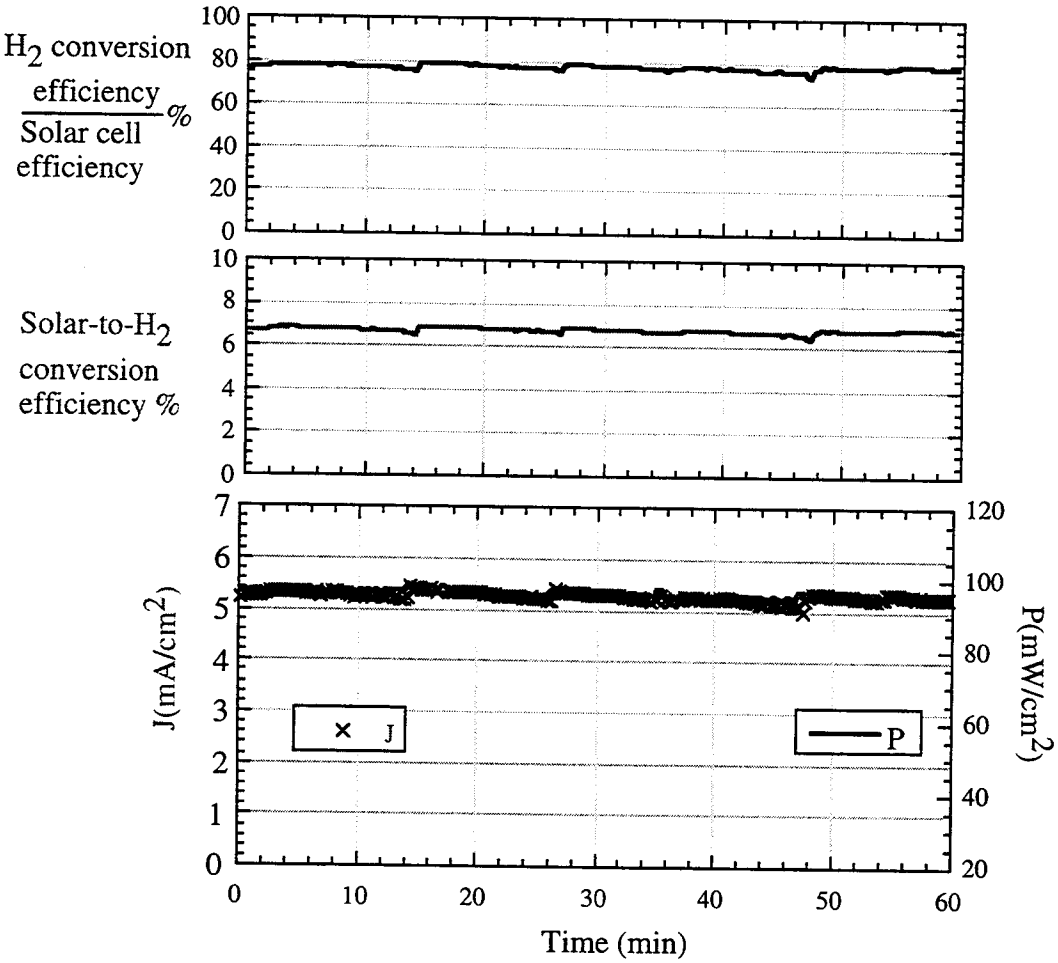
H2 conversion efficiency / Solar cell efficiency %
Solar-to-H2 conversion efficiency %
J(mA/cm2)
P(mW/cm2)
J
P
Time (min)

Figure 16